The Journal of Infectious Diseases

MAJOR ARTICLE

Batf3-Dependent Intestinal Dendritic Cells Play a Critical Role in the Control of *Cryptosporidium parvum* Infection

Laurent Potiron,[1] Sonia Lacroix-Lamandé,[1] Mathilde Marquis,[1] Yves Levern,[2] Geneviève Fort,[1] Isabelle Franceschini,[3] and Fabrice Laurent[1]

[1]INRA, Université François Rabelais de Tours, Centre Val de Loire, UMR1282 ISP, laboratoire Apicomplexes et Immunité Mucosale, [2]INRA, Université François Rabelais de Tours, Centre Val de Loire, UMR1282 ISP, Service de cytométrie, and [3]INRA, CNRS, Université François Rabelais de Tours, Institut Français du Cheval et de l'Equitation, Centre Val de Loire, UMR 85 PRC, Nouzilly France

Understanding the protective immune response to *Cryptosporidium parvum* infection is of critical importance to reduce the widespread impact caused by this disease in young individuals. Here, we analyzed the various subsets of CD103$^+$ and CD103$^-$ intestinal dendritic cells (DCs) of wild-type and Batf3$^{-/-}$ neonatal mice at homoeostasis and investigated their role during infection. Neonatal Batf3$^{-/-}$ mice had a low CD103$^+$/CD103$^-$ DC ratio, resulting in higher susceptibility to the acute phase of the infection and they could not cure the infection. Early during infection, CD103$^-$ DCs of Batf3$^{-/-}$ neonates had a lower ability to produce interleukin-12 than their wild-type littermates and lower levels of interferon-gamma mRNA were detected in the infected mucosa. Amplification of CD103$^+$ DCs in Batf3$^{-/-}$ neonates prior to infectious challenge reduced their susceptibility to infection. CD103$^+$ DCs thus outperform CD103$^-$ DCs in controlling *C. parvum* infections and represent a primary target of host-directed immunotherapies dedicated to neonates.

Keywords. dendritic cells; neonatal mice; *Cryptosporidium parvum*; intestine; innate immunity.

Cryptosporidium infection is a major threat for infants and immunocompromised individuals in impoverished and developing countries, where the disease is further amplified by malnutrition [1]. The high prevalence of *Cryptosporidium* infection in a broad range of young animals worldwide, including livestock, also contributes to human contamination by the zoonotic species *C. parvum*. The immaturity of the intestinal immune system of young individuals contributes to their higher susceptibility to infection [2, 3]. Neonates possess a thinner mucus layer, a reduced number of Paneth and immune cells, and phenotypic and functional differences of immune cells. Deciphering the immune response during cryptosporidiosis in young individuals is therefore a prerequisite for the development of dedicated host-targeted therapies.

We and others and have highlighted the major role of innate immunity in controlling the acute phase of *C. parvum* infection, whereas adaptive immunity is required to definitively clear the infection [4, 5]. Despite their importance in the intestinal immune response, the role of mononuclear phagocytes during cryptosporidiosis remains insufficiently explored. We previously demonstrated the key importance of CD11c$^+$ cells during cryptosporidiosis using the conditional mouse depletion model, CD11c-DTR [4]. Many types of mononuclear phagocytes express CD11c, including monocytes, macrophages, and dendritic cells (DCs). In addition to the first identified bona fide CD103$^+$ intestinal DC population, a CD103$^-$ DC population, lacking macrophage markers (F4/80, CD64), was recently described. Two subsets can be distinguished in each of these populations, based on expression of the panmyeloid marker CD11b. CD103$^-$ DCs are present in both the murine and human intestine and develop from DC-committed precursors and induce interleukin-17 (IL-17) production by T cells [6, 7]. These CD103$^-$CD11b$^+$ cells are also bona fide DCs that migrate in pseudoafferent lymph after activation and expand in response to fms-like tyrosine kinase 3 ligand (Flt3L) [6]. We have shown that neonatal CD103$^+$ DCs are amplified in the intestine of neonatal mice in response to Flt3L administration [4]. In addition, we previously demonstrated that repeated Flt3L administration to neonates increases their resistance to *C. parvum* [4]. Given that Flt3L governs the differentiation and proliferation of CD103$^+$ and CD103$^-$ populations, it is of major importance to investigate their relative contribution to the protective response against *C. parvum*. DC development is guided by lineage-restricted transcription factors, such as IRF8, E2-2, and Batf3 [8]. We therefore used the Baft3$^{-/-}$ mouse model, which is deficient in CD103$^+$CD8α$^+$/CD11b$^-$ DCs, to facilitate our investigation.

Here, we describe the various populations and subsets at homeostasis and during infection and show that Baft3 deficiency has direct consequences in adult and neonatal mice, increasing their susceptibility to *C. parvum* infection. The proportions and nature of the CD103$^+$ and CD103$^-$ DC populations present in wild-type (WT) and Batf3$^{-/-}$ mice differ significantly. Our results do not support a decisive role for CD103$^-$ DCs,

Received 3 July 2018; editorial decision 24 August 2018; accepted 30 August 2018; published online September 10, 2018.

Presented in part: Apicowplexa, 11–14 October 2017, Madrid, Spain.

Correspondence: F. Laurent, PhD, INRA Centre Val de Loire, UMR1282 Infectiologie et Santé Publique, Laboratoire Apicomplexes et Immunité Mucosale, 37380 Nouzilly, France (fabrice.laurent@inra.fr).

The Journal of Infectious Diseases® 2019;219:925–35

DOI: 10.1093/infdis/jiy528

which predominate in Baft3$^{-/-}$ neonates and have a lower ability to produce IL-12. Conversely, our results highlight the key role of CD103^{+} DCs in controlling *C. parvum* development in neonates.

MATERIALS AND METHODS

Mouse Models and Ethics Statement

Batf3$^{-/-}$ mice on a C57BL/6 genetic background were initially purchased from the Jackson Laboratory and acclimated and maintained in animal facilities at the Plateforme d'Infectiologie Expérimentale de Tours (PFIE). WT C57BL/6 mice were initially purchased from Janvier Labs and acclimated and maintained under similar conditions. All experiments were conducted in the facilities of the PFIE, UE-1277, INRA Centre Val de Loire, Nouzilly, France, in accordance with the guidelines of the directive 2010/63/EU of the European Parliament and of the Council. All experimental procedures (APAFIS#284; APAFIS#5261; APAFIS#01349.01) were approved by the Loire Valley ethical review board (CEEA VdL, committee number 19).

The Parasite, Mouse Infection, and Treatments

The INRA *C. parvum* isolate was used for all experiments. This strain, initially isolated from an infected child on a farm [9], is maintained by regular passage in calves in our facilities and oocysts are purified according to a previously published protocol [10]. Seven-day-old mice were infected orally with 5×10^4 to 5×10^5 *C. parvum* oocysts and adult mice with 5×10^6 *C. parvum* oocysts, depending on the protocol and as stated in the figure legends. The level of infection in individual neonatal mice was assessed by determining the number of oocysts in the intestinal contents [11], whereas in adult mice, parasite load was determined in fecal pellets individually collected for 2 hours [12]. Recombinant mouse IL-12 (Peprotech) was administered daily to Batf3$^{-/-}$ neonatal mice intraperitoneally from 3 to 6 days of age, preceding infection by *C. parvum* at 7 days of age. A mock treatment with saline solution was administered to a second group of Batf3$^{-/-}$ neonatal mice as a control.

Cell Isolation and Flow Cytometry

Intestinal epithelial cells (IEC) and lamina propria cells were isolated from the distal small intestine of neonates as described previously [4]. For flow cytometry analyses and cell sorting, IEC were gated among viable EpCam^{+} cells, and DCs were first gated from viable CD11c^{+}MHCII^{+}CD64^{-} cells and further selected into populations and subsets with CD103 and CD11b markers. The following antibodies were used: anti-CD16/CD32 (2.4G2), anti-CD45 (30-F11), anti-CD11c (N418), anti-IA/IE (2G9), anti-Ly6G (1A8), anti-CD103 (2E7), anti-CD64 (TREA286), anti-CD11b (M1/70), and anti-EpCAM (G8.8). Cells were analyzed on a LSR Fortessa flow cytometer (Becton Dickinson) or sorted with a MoFlo cell sorter (Beckman Coulter).

RNA Extraction and Quantitative RT-PCR

Total RNA was extracted from IEC isolated from the distal small intestine of individual neonatal mice and purified using TRIZOL reagent. Quantitative reverse transcription polymerase chain reaction (qRT-PCR) was performed as previously described [13]. Pools of cells from 3 neonates were constituted, as only a low number of DCs can be extracted from the intestine of neonates, and 10^3 CD103^{+} or CD103^{-} DCs were used to perform qRT-PCR, as previously published [14]. Expression levels were calculated using the formula $2(-\Delta Ct)$, where ΔCt = Ctgene − average Ct housekeeping. Genes TATA box binding protein (*TBP*) and peptidylprolyl isomerase A (*PPia*) served as internal standards for normalization.

Primer sequences for the target and housekeeping genes (*PPia*, *TBP*) have been previously published [4, 13] or are provided here. IFN regulatory factor 4 (*IRF4*): forward 5′-CTACCCCATGACAGCACCTT-3′, reverse 5′-CCAAACGTCACAGGACATTG-3′; *IRF8*: forward 5′-AAGTGACTGACCGGTCCCA-3′, reverse 5′-AACTTCGCTCATGCAGCCT-3′; indoleamine-pyrrole 2,3-dioxygenase (*IDO1*): forward 5′-ATCTCCTGGATGAGAAAGGCAAGG-3′, reverse 5′-TGTTGTGGAAGAACTCTGGGAAGG-3′.

Protein Extraction and Western Blot

IEC were isolated at 13 days of age from the distal small intestine of sham and *C. parvum* infected neonates. Proteins were extracted from 3 pools of IEC from 2 or 3 neonates per pool, as previously published [15]. Sodium dodecyl sulfate polyacrylamide gel electrophoresis was performed on 30 µg protein. The quantity of IDO1 was expressed relative to β-actin content.

Immunofluorescence Staining

Immunofluorescence histology was performed as previously described [4]. Briefly, ileal tissue isolated from neonatal or adult mice was fixed in antigenfix, washed twice with phosphate-buffered saline, incubated 3 hours in 30% sucrose, and finally frozen in OCT. Sections, 7-µm thick, were stained with primary and secondary antibodies in 1% bovine serum albumin /0.1% Triton. Slides were stained with Hoechst and mounted in Fluoromount medium (Interchim). Images were prepared using Axiovision software (Zeiss). Antibodies used for immunohistochemistry were an anti-EpCAM and a rat polyclonal anti-*C. parvum* antibody generated against an antigenic extract of *C. parvum* oocysts.

Statistical Analyses

Statistical analyses were performed using GraphPad Prism7 software. Two-group analyses were performed using the Mann–Whitney nonparametric *t* test. For multigroup analyses, we used the nonparametric Kruskal–Wallis followed by Dunn multiple comparison. For all analyses, a *P* value of .05 was considered significant.

RESULTS

Batf3$^{-/-}$ Mice Are More Susceptible to *C. parvum* Infection Than Wild-Type Mice

Batf3$^{-/-}$ mice are known to present deficiencies in the CD103^{+} CD11b^{-} DC subset important for the control of *Toxoplasma gondii* and *Leishmania major* infections [16, 17]. Parasite load was evaluated in the content of the small intestine of infected WT and Batf3$^{-/-}$ neonates. The kinetics of infection appeared to be similar for both strains of mice, with a peak of infection at 6 days postinfection (dpi), preceding parasite control (Figure 1A). However, the parasite developed more efficiently in Batf3$^{-/-}$ neonatal mice, which had 4-fold more parasites in the luminal content than their WT counterparts at 6 dpi (Figure 1B). The higher level of infection in the ileum of Batf3$^{-/-}$ neonatal mice was confirmed by immunohistology (Figure 1C and 1D).

We investigated whether neonatal WT and Batf3$^{-/-}$ mice fully control the infection by analyzing the parasite load 5 weeks postinfection. As expected, we detected no oocysts in the feces of WT, whereas a few oocysts were consistently detected in the feces of Batf3$^{-/-}$ mice (data not shown). Thus, infected neonatal Batf3$^{-/-}$ mice remain infected by *C. parvum* for at least 5 weeks, as further confirmed by immunohistology, revealing areas of the intestine that were clearly infected by *C. parvum* (Figure 1E).

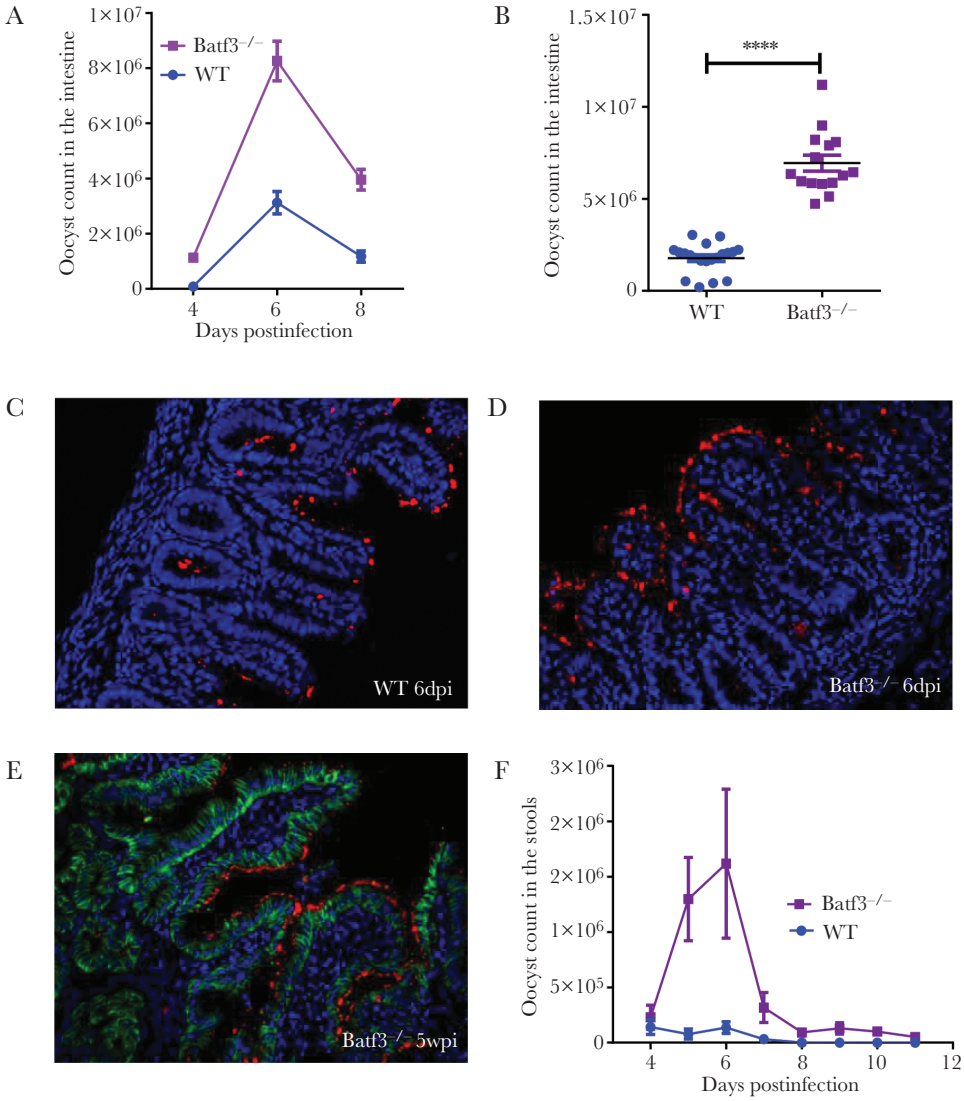

Figure 1. Susceptibility of neonatal and adult Batf3$^{-/-}$ mice to *Cryptosporidium parvum* infection. *A*, Seven-day-old neonatal mice were inoculated with 5×10^5 oocysts of *C. parvum* and the parasite load of each neonate analyzed at 4, 6, and 8 days postinfection (dpi; median ± SEM, n = 7–11 per day per group). *B*, Similar experiment as in (*A*) performed with a larger number of neonates per group at 6 dpi (n = 16–20). Each symbol represents 1 animal (median ± SE; **** Mann–Whitney statistical test $P < .0001$). Immunohistochemistry of the ileum of wild-type (WT) neonatal mice at 6 dpi (*C*), Batf3$^{-/-}$ neonatal mice at 6 dpi (*D*), and 5 weeks later (*E*). *C. parvum* stained in red with a rat polyclonal anti-*C. parvum* antibody, nuclei stained in blue with Hoechst dye, and EpCAM stained in green. *F*, WT and Batf3$^{-/-}$ adult mice (8 weeks old) were infected with 5×10^6 oocysts of *C. parvum*. Oocyst excretion was quantified by daily individual fecal collection (median ± SEM, n = 5 per group).

We next investigated the ability of *C. parvum* to develop in adult Batf3$^{-/-}$ mice. As expected, WT mice were strongly resistant to the infection, with barely detectable oocysts produced in the feces. In contrast, Batf3$^{-/-}$ mice presented a clear infection that peaked at 6 dpi, followed by a decrease of parasite load, although it was not complete, as a low level of parasites were still detected at 11 days dpi (Figure 1F). Overall, these results show that Batf3$^{-/-}$ deficiency clearly alters both the very early step of parasite control and definitive control of the infection.

Batf3$^{-/-}$ Deficiency in Neonatal Mice Affects Both Intestinal CD103^{+} DC Subsets

Genetic alterations may have different consequences in neonates than adults. Thus, we compared CD103^{+} and CD103^{-} DC subsets in the neonatal mouse intestine to that of adults. In adults, Batf3 deficiency resulted in a severe reduction of intestinal CD103^{+} CD11b^{-} DCs, as expected, but also a large increase in the proportion of CD103^{-} DCs (Figure 2A).

The situation in Batf3$^{-/-}$ neonates differed from that of adults, as both CD103^{+} DC subsets were affected by Batf3 deficiency

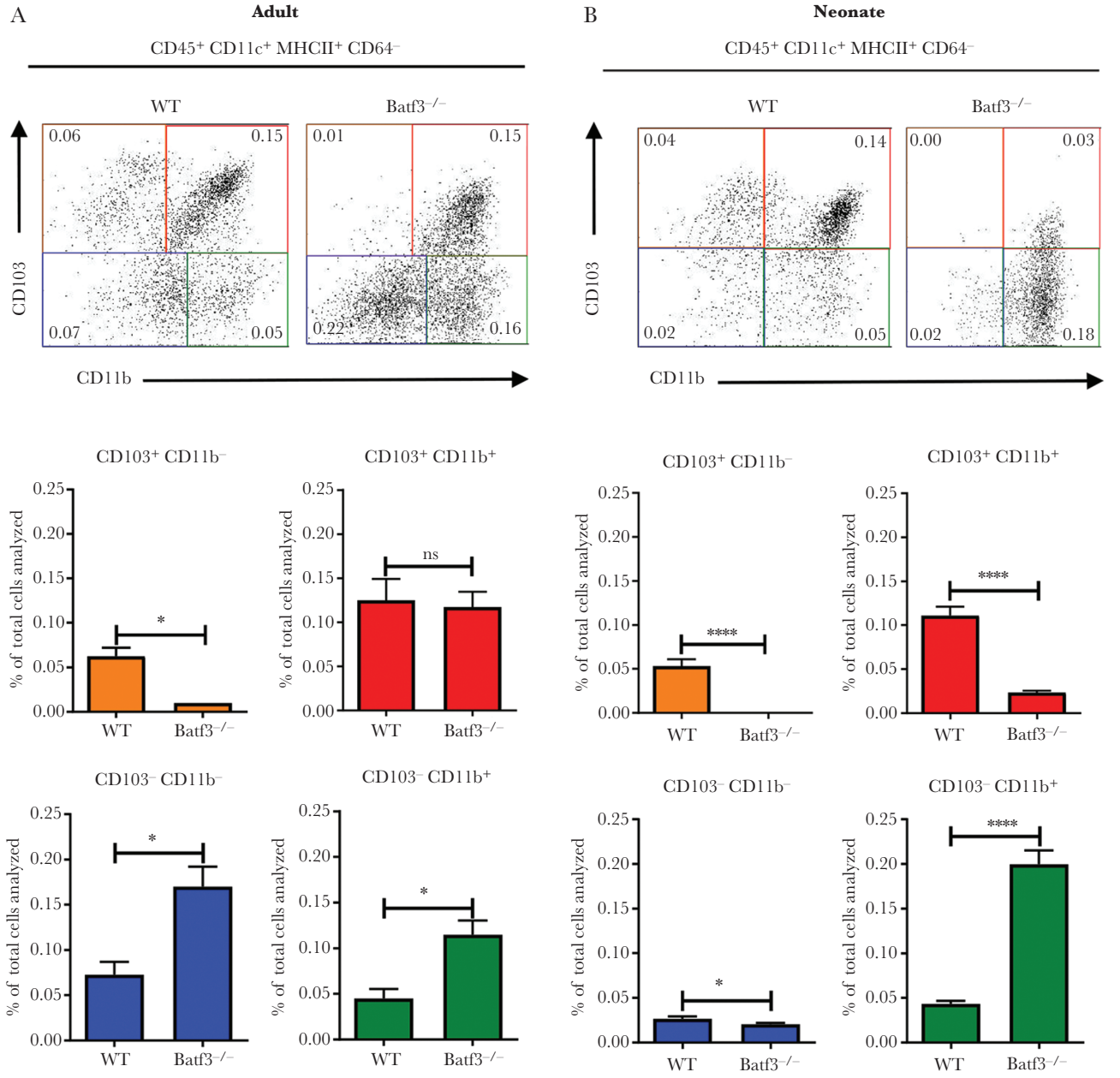

Figure 2. Frequency of intestinal dendritic cell (DC) subsets in adult and neonatal wild-type (WT) and Batf3$^{-/-}$ mice. CD45^{+}CD11c^{+}MHCII^{+}CD64^{-} cells from distal small intestine of adult (*A*) and 13-day-old neonatal mice (*B*) were analyzed by flow cytometry and further gated on CD103 and CD11b expression to analyze the 4 DC subsets. Neonates (n = 9–14); adults (n = 6). Mann–Whitney statistical test ****$P < .0001$; *$P < .05$; ns, not significant.

(Figure 2B). The CD11b$^-$ subset was absent in the intestine of Batf3$^{-/-}$ neonates and the frequency of the CD11b$^+$ subset was reduced by 5-fold. In contrast, the CD103$^-$CD11b$^+$ cells were 5-fold more abundant in the intestinal mucosa of Batf3$^{-/-}$ mice and constituted the major DC subset. Importantly, the percentage of the different DC populations (CD103$^+$, CD103$^-$) among CD45$^+$ lamina propria cells in uninfected neonates were not significantly different between WT (mean 2.58% ± 0.77%) and Batf3$^{-/-}$ mice (mean 2.66% ± 0.66%) (Supplementary Figure 1). This suggests that the nature of the DC subsets and their respective functions, rather than the total number of DCs, is instrumental in the protection of neonates against *C. parvum*.

CD103$^+$ CD11b$^-$ DCs Are Generated in Batf3$^{-/-}$ Neonates During *C. parvum* Infection

We analyzed intestinal DC subsets at the peak of infection (6 dpi), when neonatal mice start to control the infection. In WT neonates, CD103$^+$ DCs predominated in the small intestine (Figure 3A) and mesenteric lymph nodes (MLN) (Figure 3B), but after infection, the distribution of the 4 DC subsets was more evenly balanced in the intestine. Infected Batf3$^{-/-}$ neonatal mice showed the emergence of CD103$^+$CD11b$^-$ DCs in the intestine, which were undetectable at homeostasis (Figure 3A). This subset represented more than a quarter of the DCs present in the MLN of these animals at 6 dpi (Figure 3B). Thus, *C. parvum* infection induces the generation of CD103$^+$CD11b$^-$ DCs in Batf3$^{-/-}$ neonates as previously observed for Batf3$^{-/-}$ mice infected by *T. gondii* [16]. The proportion of CD103$^+$ DCs dramatically changed in the MLN of Batf3$^{-/-}$ neonatal mice during infection, rising from 3% to 50%, to reach proportions similar to those of infected WT mice.

Although it is not possible to analyze the afferent lymph in neonates, all DC subsets increased in number in the MLN during infection, suggesting that both CD103$^+$ and CD103$^-$ DC subsets migrate from the intestine to the draining lymph nodes.

Batf3 Deficiency Does Not Alter the Proportion of Intestinal Monocyte-Macrophage Subsets in Neonatal Mice

We showed that Batf3 deficiency has a broader effect in neonates than adults, affecting both CD103$^+$ DC subsets. We therefore verified the proportions of CD64$^+$Ly6c$^-$ resident macrophages and recently recruited CD64$^+$Ly6c$^+$ monocytes/macrophages in the distal small intestine of Batf3$^{-/-}$ neonatal mice by flow cytometry (Supplementary Figure 2A). There was no difference in the proportion of these populations between 13-day-old Batf3$^{-/-}$ neonatal mice and WT age-matched controls at homeostasis. At the peak of infection, CD64$^+$ Ly6c$^+$ inflammatory monocytes/macrophages were strongly recruited to the infected mucosa [15] in similar proportions in both strains of mice (Supplementary Figure 2B), revealing no consequences on monocyte/macrophage recruitment and differentiation.

IFN-γ and IDO1 mRNA Upregulation Is Reduced in the Early Phase of the Infection in Batf3$^{-/-}$ Neonates

We next investigated the reason for the difference in the susceptibility of Batf3$^{-/-}$ and WT neonatal mice. Interferon-gamma (IFN-γ) is a key effector cytokine for controlling *C. parvum* replication in intestinal epithelial cells [4, 10, 18]. IFN-γ was upregulated 150-fold in the infected neonatal mucosae at 6 dpi (Figure 4A). We investigated the consequences of local IFN-γ production on IEC by assessing IDO1 expression, an enzyme that catabolizes tryptophan and thus limits the growth of auxotrophic pathogens, such as *T. gondii* [19]. IDO1 protein levels were higher in IECs isolated from infected animals (Figure 4B) and its strong dependence on IFN-γ for its expression was definitively confirmed by the 200-fold higher IDO1 upregulation observed during infection in IECs isolated from WT mice relative to those from IFN-γ$^{-/-}$ neonatal mice (Figure 4C).

Batf3$^{-/-}$ neonatal mice were more heavily infected than WT neonates as soon as 4 dpi. The comparison of cytokine production between these 2 mouse strains during this early step of infection may therefore be difficult to interpret. We therefore infected neonatal mice with several inoculation doses of oocysts and selected a 100-fold lower infectious dose for the Batf3$^{-/-}$ neonates. Under this experimental condition, we were able to select animals with similar parasite loads in both groups at 4 dpi (Figure 4D, dotted frame). With a similar parasite load, IFN-γ and IDO1 were 20- and 12-fold more highly upregulated, respectively, in WT than Batf3$^{-/-}$ neonates (Figure 4D, right panels).

CD103$^+$ DCs Produce IL-12 More Efficiently Than CD103$^-$ DCs in Infected Neonates

We investigated the respective contribution of CD103$^+$ and CD103$^-$ DCs to IFN-γ and IL-12 production in WT and Batf3$^{-/-}$ neonates. Further analyses of CD11b$^+$ and CD11b$^-$ subsets were not feasible due to the limited number of DCs that can be isolated from the distal small intestine of neonatal mice for some subsets. WT and Batf3$^{-/-}$ neonatal mice were infected at 7 days of age with 5×10^6 and 5×10^4 oocysts of *C. parvum*, respectively, to obtain a similar parasitic load at 4 dpi and CD103$^+$ and CD103$^-$ DCs were isolated from the distal small intestine. CD103$^+$ DCs from both WT and Batf3$^{-/-}$ neonatal mice are most likely better producers of functional IL-12 due to their higher expression of both IL-12p40 and IL-12p35 chains, which make up the heterodimeric IL-12p70 (Figure 5A). IFN-γ was expressed at similar levels by CD103$^+$ and CD103$^-$ DCs, but DCs isolated from infected WT neonates expressed significantly higher levels of IFN-γ. Conventional DC (cDC) subsets arise via distinct networks of transcription factors involving IRF4 and IRF8, and are specialized for unique functional responses. IRF8 was expressed at higher levels in CD103$^+$ DCs isolated from infected WT neonates (Figure 5B), revealing their higher potential to promote Th1 responses. Conversely, IRF4,

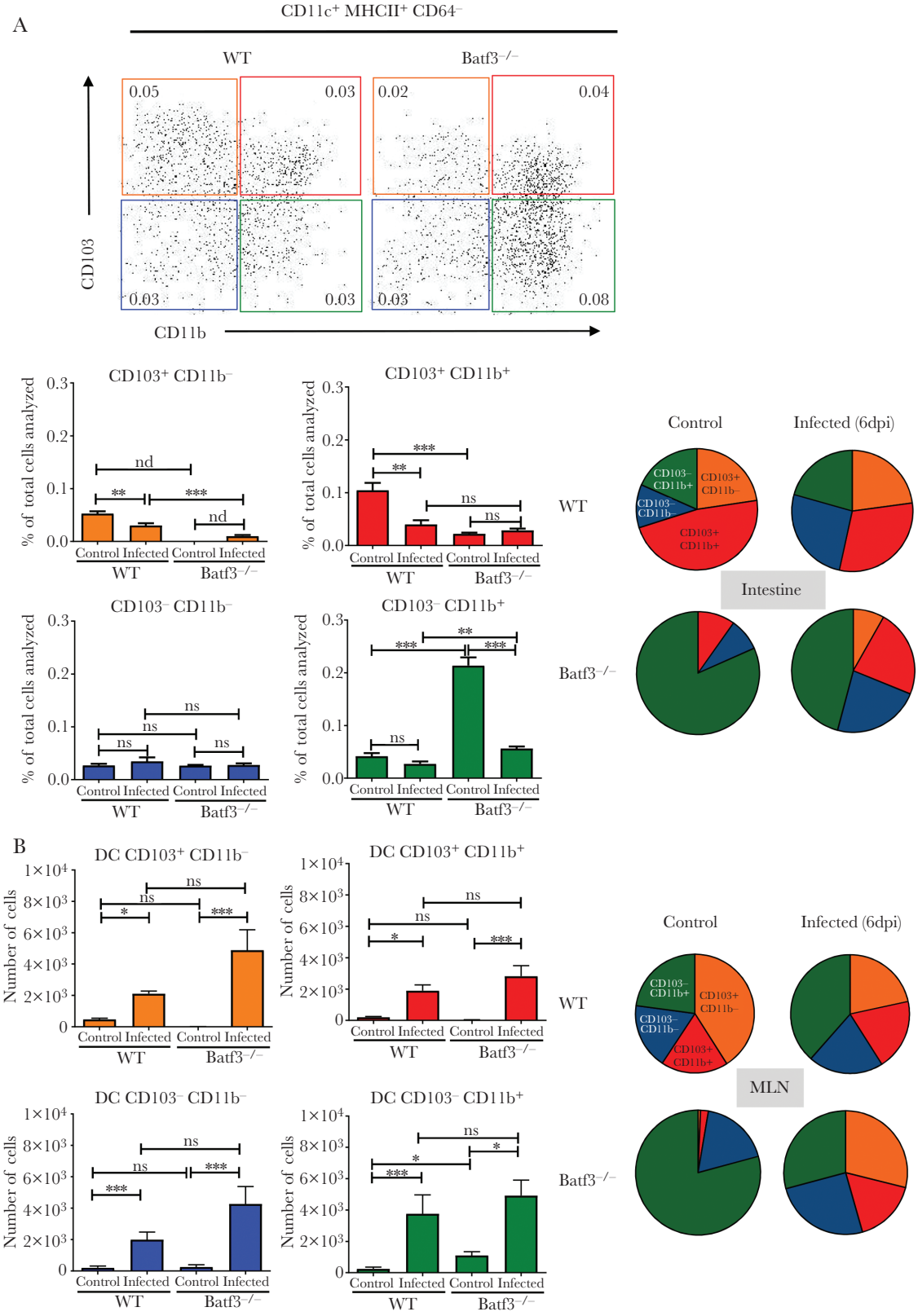

Figure 3. Evolution of dendritic cell (DC) subsets in the intestine and mesenteric lymph nodes (MLN) during *Cryptosporidium parvum* infection of neonates. Neonatal wild-type (WT) and Batf3$^{-/-}$ mice were infected, or sham infected, at 7 days of age with 5×10^5 oocysts of *C. parvum*. *A*, Intestine and (*B*) MLN were removed at 6 days postinfection (dpi) and DC cell subsets analyzed by flow cytometry. *A*, Representative flow cytometry chart and proportion of the various subsets in the intestine of control and infected mice (WT and Baft3$^{-/-}$) are presented on bar graphs and pie charts to facilitate comparative analyses. *B*, Proportion of the various subsets in the MLN of control and infected mice (WT and Baft3$^{-/-}$) are presented in the bar graph and pie chart. Statistical analyses were performed with the Kruskal-Wallis nonparametric test followed by Dunn multiple comparison ***$P < .005$; **$P < .01$; *$P < .05$; ns, not significant. Data are from 2 representative experiments (n = 6–12).

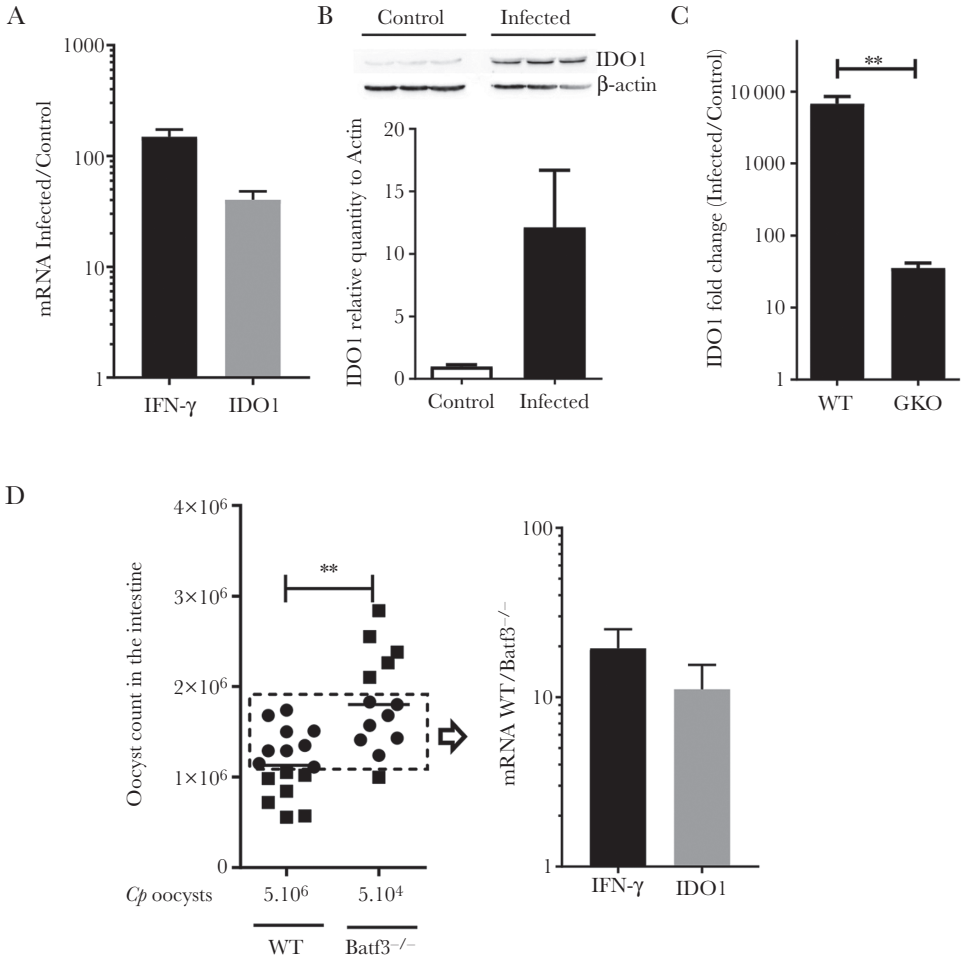

Figure 4. Interferon-gamma (IFN-γ) and indoleamine-pyrrole 2,3-dioxygenase (IDO1) expression in the distal small intestine of wild-type (WT) and Batf3$^{-/-}$ neonates infected by *Cryptosporidium parvum* (Cp). *A*, WT neonatal mice were infected with 5×10^5 oocysts of *C. parvum* at 7 days of age and RNA from ileal mucosae isolated at 6 days postinfection. Quantitative reverse transcription polymerase chain reaction (qRT-PCR) was performed to evaluate IFN-γ and IDO1 expression (n = 7 per group). *B*, IEC were isolated from the distal part of the small intestine at 13 days of age from sham-infected animals or animals infected 6 days before with 5×10^5 oocysts of *C. parvum*. Western blotting was performed with 3 samples in each group, corresponding to pools from 2 to 3 neonates. The quantity of IDO1 is expressed relative to β-actin content. *C*, WT and IFN-γ$^{-/-}$ (GKO) neonatal mice were infected at 7 days of age with 5×10^5 oocysts of *C. parvum* and IEC isolated at 6 dpi. qRT-PCR was performed to evaluate IDO1 expression in both groups of mice (n = 6 per group; Mann–Whitney statistical test $^{**}P < .005$). *D*, WT and Batf3$^{-/-}$ neonatal mice were infected at 7 days of age with 5×10^6 and 5×10^4 oocysts, respectively. The parasite load in the intestine was determined for each neonate (n = 16 per group) at 4 dpi and a small piece of ileal tissue used for RNA extraction for qRT-PCR analyses (n = 7–8 per group). IFN-γ and IDO1 mRNA expression (right panel) was analyzed only in animals presenting a similar parasite load ($1.2–1.8 \times 10^6$) for both strains (black dots in the area of selection, left panel).

an important transcription factor that drives DCs to promote Th17 differentiation [20], was expressed at higher levels in DCs from infected Batf3$^{-/-}$ neonatal mice (Figure 5B).

Repeated IL-12 Administration to Neonatal Mice Compensates for Altered Development of CD103 DCs in Batf3$^{-/-}$ Mice

Tussiwand et al [21] identified an alternative, Batf3-independent pathway in mice for CD103$^+$CD8α$^+$CD11b$^-$ DC development that operates during infection with intracellular pathogens. This pathway is mediated by cytokines (IL-12, IFN-γ) and transcription factors (Batf, Batf2). We investigated the consequences of 4 rounds of IL-12 administration to Batf3$^{-/-}$ neonatal mice from 3 to 6 days of age on DC subset development and susceptibility to subsequent *C. parvum* infection. IL-12 treatment resulted in a clear increase of CD103$^+$ DCs and concomitant decrease of CD103$^-$ DCs in the distal small intestine of neonates (Figure 6A). CD103$^+$CD11b$^-$ DCs were the most affected, showing a 7-fold increase, whereas CD103$^+$CD11b$^+$ DCs increased 2.5-fold. Neonatal Batf3$^{-/-}$ mice treated with IL-12 at 7 days of age, prior to *C. parvum* infection, showed a significant reduction in parasite load at 6 dpi (Figure 6B), supporting a key role of CD103$^+$ DCs, particularly CD103$^+$CD11b$^-$ DCs, in the control of the early step of the infection.

DISCUSSION

In the intestine, mononuclear phagocytes form a dense interconnected network of recently infiltrated monocytes, macrophages, and DCs. Four different DC subsets have been described

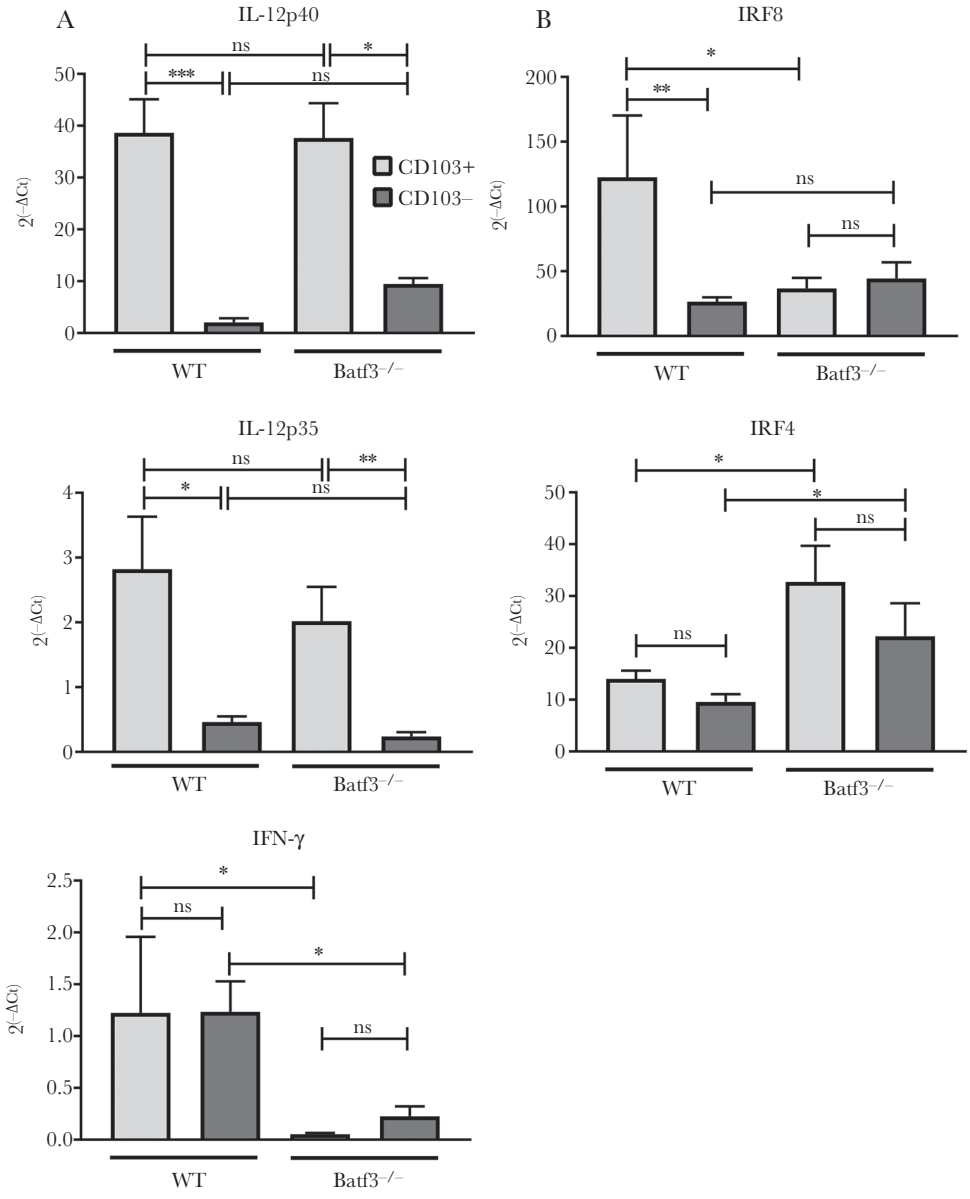

Figure 5. Cytokine and transcription-factor expression in CD103$^+$ and CD103$^-$ dendritic cells (DCs) from wild-type (WT) and Batf3$^{-/-}$ neonates infected by *Cryptosporidium parvum*. Neonatal WT and Batf3$^{-/-}$ mice were infected at 7 days of age with 5×10^6 and 5×10^4 oocysts of *C. parvum*, respectively. DCs were isolated from the distal part of the small intestine at 4 days postinfection and EpCAM$^-$CD11c$^+$MHCII$^+$CD64$^-$CD103$^+$ and EpCAM$^-$CD11c$^+$ClassII$^+$CD64$^-$CD103$^-$ populations sorted by flow cytometry. The cells isolated from 3 neonates were pooled to obtain a sufficient number of cells. *A*, RNA was extracted from each pool (n = 8 for each condition) and quantitative reverse transcription polymerase chain reaction (qRT-PCR) performed for the selected cytokines and (*B*) transcription factors. Values (n = 8) represent the mean ± SEM. Statistical analyses were performed with the Kruskal–Wallis nonparametric test followed by Dunn multiple comparison. *$P < .05$; **$P < .005$; ***$P < .0005$; ns, not significant.

in the intestine in adults, CD103$^+$CD11b$^-$, CD103$^+$CD11b$^+$, CD103$^-$CD11b$^+$, and CD103$^-$CD11b$^-$, the latter being less represented [22]. The 3 major subsets have migratory properties and continuously migrate through the lymphatics to the MLNs [6].

We investigated the relative importance of these DC subsets during *C. parvum* infection in neonatal mice using Batf3$^{-/-}$ mice, known to present a major defect in the CD103$^+$CD11b$^-$ population. Batf3$^{-/-}$ neonatal mice became more heavily infected than their WT littermates. Further experiments revealed that a higher infectious dose of 2 $\log_{10}$ was required to reach an equivalent parasite load in WT mice at 4 dpi. Five weeks after being infected as neonates, IECs of Batf3$^{-/-}$ mice were still infected, revealing the importance of Batf3-dependent DCs in the definitive control of the infection. In addition, adult mice, which are strongly resistant to *C. parvum* infection, were clearly infected by *C. parvum* when deficient for Batf3. Overall, these data clearly show the key importance of Batf3-dependent DCs during the acute phase and for the definitive control of the infection. Batf3 deficiency in neonates not only affected intestinal CD103$^+$CD11b$^-$ DCs, as in adults, but also the CD103$^+$CD11b$^+$

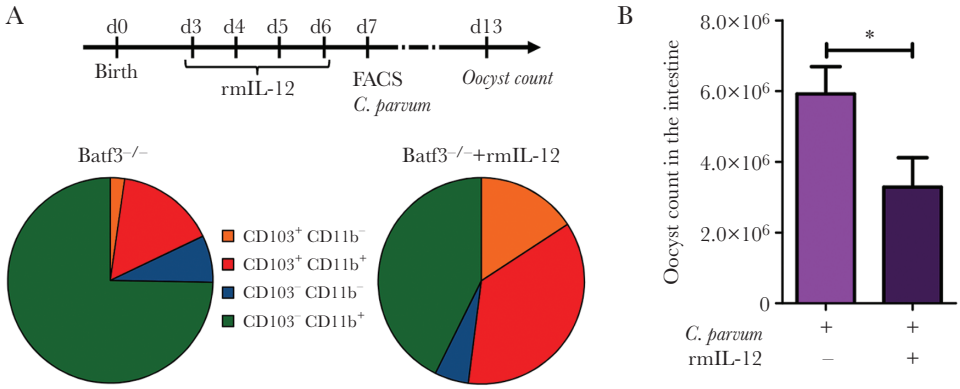

Figure 6. Effect of interleukin-12 (IL-12) injection on the frequency of intestinal dendritic cell (DC) subsets and susceptibility to infection of neonatal Batf3$^{-/-}$ mice. Batf3$^{-/-}$ deficient mice were injected intraperitoneally with 0.25 µg rmIL-12 at 3, 4, 5, and 6 days of age or mock treated with saline solution in the same conditions. *A,* DC subsets in the intestine of IL-12 treated neonatal mice and age-matched controls were analyzed by flow cytometry (FACS) at 7 days of age. The pie chart represents the frequency of the 4 DC subsets in each group (n = 8–9 mice per group). *B,* The same experiment was continued by infecting both groups with 5×10^5 oocysts of *Cryptosporidium parvum* and analyzing the parasite load at the peak of infection (6 days postinfection, 13 days of age). Statistical analyses were performed with the Mann–Whitney test. *$P < .05$. (n = 8–9 mice per group).

subset, although to a lesser extent. The total number of DCs in these animals was no different from that in WT controls, suggesting that CD103$^-$ DCs may represent an undifferentiated population of CD103$^+$ DCs and that Batf3 participates in their differentiation. However, intestinal CD103$^-$CD11b$^+$ DCs have been previously shown to produce IL-23 in response to bacterial flagellin [23] and are also able to induce IL-17 production by T cells [7]. Alternatively, this may also result from a compensatory mechanism triggered by the presence of a limited number of CD103$^+$ DCs, leading to increased representation of CD103$^-$ DCs in the lamina propria. It is still unclear whether these subsets truly represent different populations or rather distinct developmental or activation stages [24].

Compensatory DC development, mediated by Batf and Batf2 transcription factors, has been observed in inflammatory conditions, in which the cytokine IL-12 plays a critical role [21]. Indeed, we were able to partially reverse the Batf3 defect in CD103$^+$ DCs by injecting neonatal mice with IL-12, rendering the animals less susceptible to a subsequent *C. parvum* challenge. IL-12 induced an increase in the proportion of CD103$^+$CD11b$^-$ and CD103$^+$CD11b$^+$ subsets, revealing that these subsets depend on several members of the Batf family transcription factors for their development in neonates. CD103$^+$ DCs that produce a higher level of IL-12 were 4 times more numerous in WT than Batf3$^{-/-}$ neonates, consistent with their better ability to control *C. parvum* infection. We confirmed the ability of CD103$^+$ DCs to produce IFN-γ in response to *C. parvum* infection in WT neonates [4] and extended this previous observation to CD103$^-$ DCs, which produced similar levels. In addition, DCs from Batf3$^{-/-}$ neonatal mice had a lower ability to produce IFN-γ.

Therefore, in the intestine, the 20-fold higher expression of IFN-γ by WT than Batf3$^{-/-}$ neonates during early infection (4 dpi) may result from DCs, but this does not exclude the contribution of other cellular sources activated by IL-12 produced by CD103$^+$ DCs, which predominate in WT neonates. Type 1 innate lymphoid cells are good candidates for such innate IFN-γ production, although they are only present in very low numbers in the neonatal intestine [25], but this still needs to be demonstrated. Locally released IFN-γ is critical for controlling *C. parvum* development in enterocytes. IFN-γ–dependent genes, such as *IDO1*, were induced at lower levels in IECs isolated from Batf3$^{-/-}$ mice during early infection. IDO1 activation induces tryptophan starvation, an efficient mechanism for controlling *T. gondii* growth [19]. However, Choudhry et al showed that *C. parvum* can block IDO expression in the human epithelial cell lines HT29 and Caco-2 [26]. This escape mechanism and its efficacy in controlling IDO expression is yet to be demonstrated in vivo.

Overall, our data clearly emphasize the preponderant role of the transcription factor Batf3 and CD103$^+$ DCs, particularly DC103$^+$CD11b$^-$ DCs, (1) in the resolution of the acute phase of the infection through cytokine secretion, as well as (2) for the complete clearance of the parasite, which requires the engagement of adaptive immunity and functional conventional T cells [4, 27]. It was recently reported that intestinal Batf3-dependent DCs are required for optimal antiviral T-cell responses in neonatal mice against rotavirus infection, the major cause of childhood gastroenteritis worldwide [28]. We have previously shown that immune-stimulation strategies applied to neonates is an efficient method to strengthen their ability to control cryptosporidiosis [11, 29]. In this context, CD103$^+$CD11b$^-$ DCs represent a primary target for the application of immune-stimulation strategies to neonates for reducing the burden of neonatal enteric diseases.

Supplementary Data

Supplementary materials are available at *The Journal of Infectious Diseases* online. Consisting of data provided by the authors to benefit the reader, the posted materials are not copyedited and are the sole responsibility of the authors, so questions or comments should be addressed to the corresponding author.

Notes

Acknowledgments. We are grateful to the scientific and animal staff of the Plate-Forme d'Infectiologie Expérimentale: PFIE, UE-1277, INRA Centre Val de Loire, Nouzilly, France. PFIE is part of EMERG'IN, the national infrastructure for the control of animal and zoonotic emerging infectious diseases through in vivo investigation. We are also especially thankful to the animal technicians in charge of rearing the mice (Corinne Beauge and her team) and for their help in the follow-up of the experiments (Edouard Guitton and his team, in particular Fanny Sarce).

Financial support. This work was supported by the Institut National de la Recherche Agronomique.

Potential conflicts of interest. All authors: No reported conflicts of interest. All authors have submitted the ICMJE Form for Disclosure of Potential Conflicts of Interest. Conflicts that the editors consider relevant to the content of the manuscript have been disclosed.

References

1. Costa LB, JohnBull EA, Reeves JT, et al. *Cryptosporidium*-malnutrition interactions: mucosal disruption, cytokines, and TLR signaling in a weaned murine model. J Parasitol **2011**; 97:1113–20.
2. Hornef MW, Fulde M. Ontogeny of intestinal epithelial innate immune responses. Front Immunol **2014**; 5:474.
3. Zhang K, Dupont A, Torow N, et al. Age-dependent enterocyte invasion and microcolony formation by *Salmonella*. PLoS Pathog **2014**; 10:e1004385.
4. Lantier L, Lacroix-Lamandé S, Potiron L, et al. Intestinal CD103+ dendritic cells are key players in the innate immune control of *Cryptosporidium parvum* infection in neonatal mice. PLoS Pathog **2013**; 9:e1003801.
5. Barakat FM, McDonald V, Di Santo JP, Korbel DS. Roles for NK cells and an NK cell-independent source of intestinal gamma interferon for innate immunity to *Cryptosporidium parvum* infection. Infect Immun **2009**; 77:5044–9.
6. Cerovic V, Houston SA, Scott CL, et al. Intestinal CD103(-) dendritic cells migrate in lymph and prime effector T cells. Mucosal Immunol **2013**; 6:104–13.
7. Scott CL, Bain CC, Wright PB, et al. CCR2(+)CD103(-) intestinal dendritic cells develop from DC-committed precursors and induce interleukin-17 production by T cells. Mucosal Immunol **2015**; 8:327–39.
8. Watowich SS, Liu YJ. Mechanisms regulating dendritic cell specification and development. Immunol Rev **2010**; 238:76–92.
9. Arnaud-Battandier F, Naceri M, Fischer A, Ricour C, Griscelli C, Yvore P. Intestinal cryptosporidiosis: a new cause of diarrhea in man? Gastroenterol Clin Biol **1982**; 6:1045–6.
10. Lacroix-Lamandé S, Mancassola R, Naciri M, Laurent F. Role of gamma interferon in chemokine expression in the ileum of mice and in a murine intestinal epithelial cell line after *Cryptosporidium parvum* infection. Infect Immun **2002**; 70:2090–9.
11. Barrier M, Lacroix-Lamandé S, Mancassola R, et al. Oral and intraperitoneal administration of phosphorothioate oligodeoxynucleotides leads to control of *Cryptosporidium parvum* infection in neonatal mice. J Infect Dis **2006**; 193:1400–7.
12. Lacroix S, Mancassola R, Naciri M, Laurent F. *Cryptosporidium parvum*-specific mucosal immune response in C57BL/6 neonatal and gamma interferon-deficient mice: role of tumor necrosis factor alpha in protection. Infect Immun **2001**; 69:1635–42.
13. Guesdon W, Auray G, Pezier T, et al. CCL20 displays antimicrobial activity against *Cryptosporidium parvum*, but its expression is reduced during infection in the intestine of neonatal mice. J Infect Dis **2015**; 212:1332–40.
14. Ho V, Yeo SY, Kunasegaran K, et al. Expression analysis of rare cellular subsets: direct RT-PCR on limited cell numbers obtained by FACS or soft agar assays. Biotechniques **2013**; 54:208–12.
15. de Sablet T, Potiron L, Marquis M, Bussière FI, Lacroix-Lamandé S, Laurent F. *Cryptosporidium parvum* increases intestinal permeability through interaction with epithelial cells and IL-1β and TNFα released by inflammatory monocytes. Cell Microbiol **2016**; 18:1871–80.
16. Mashayekhi M, Sandau MM, Dunay IR, et al. CD8α(+) dendritic cells are the critical source of interleukin-12 that controls acute infection by *Toxoplasma gondii* tachyzoites. Immunity **2011**; 35:249–59.
17. Ashok D, Schuster S, Ronet C, et al. Cross-presenting dendritic cells are required for control of *Leishmania* major infection. Eur J Immunol **2014**; 44:1422–32.
18. Theodos CM, Sullivan KL, Griffiths JK, Tzipori S. Profiles of healing and nonhealing *Cryptosporidium parvum* infection in C57BL/6 mice with functional B and T lymphocytes: the extent of gamma interferon modulation determines the outcome of infection. Infect Immun **1997**; 65:4761–9.
19. Cerávolo IP, Chaves AC, Bonjardim CA, Sibley D, Romanha AJ, Gazzinelli RT. Replication of *Toxoplasma gondii*, but not *Trypanosoma cruzi*, is regulated in human fibroblasts activated with gamma interferon: requirement of a functional JAK/STAT pathway. Infect Immun **1999**; 67:2233–40.

20. Persson EK, Uronen-Hansson H, Semmrich M, et al. IRF4 transcription-factor-dependent CD103(+)CD11b(+) dendritic cells drive mucosal T helper 17 cell differentiation. Immunity **2013**; 38:958–69.
21. Tussiwand R, Lee WL, Murphy TL, et al. Compensatory dendritic cell development mediated by BATF-IRF interactions. Nature **2012**; 490:502–7.
22. Persson EK, Scott CL, Mowat AM, Agace WW. Dendritic cell subsets in the intestinal lamina propria: ontogeny and function. Eur J Immunol **2013**; 43:3098–107.
23. Kinnebrew MA, Buffie CG, Diehl GE, et al. Interleukin 23 production by intestinal CD103(+)CD11b(+) dendritic cells in response to bacterial flagellin enhances mucosal innate immune defense. Immunity **2012**; 36:276–87.
24. Sichien D, Lambrecht BN, Guilliams M, Scott CL. Development of conventional dendritic cells: from common bone marrow progenitors to multiple subsets in peripheral tissues. Mucosal Immunol **2017**; 10:831–44.
25. Fuchs A, Vermi W, Lee JS, et al. Intraepithelial type 1 innate lymphoid cells are a unique subset of IL-12- and IL-15-responsive IFN-γ-producing cells. Immunity **2013**; 38:769–81.
26. Choudhry N, Korbel DS, Edwards LA, Bajaj-Elliott M, McDonald V. Dysregulation of interferon-gamma-mediated signalling pathway in intestinal epithelial cells by *Cryptosporidium parvum* infection. Cell Microbiol **2009**; 11:1354–64.
27. Korbel DS, Barakat FM, Di Santo JP, McDonald V. CD4+ T cells are not essential for control of early acute *Cryptosporidium parvum* infection in neonatal mice. Infect Immun **2011**; 79:1647–53.
28. Sun T, Rojas OL, Li C, Ward LA, Philpott DJ, Gommerman JL. Intestinal Batf3-dependent dendritic cells are required for optimal antiviral T-cell responses in adult and neonatal mice. Mucosal Immunol **2017**; 10:775–88.
29. Lantier L, Drouet F, Guesdon W, et al. Poly(I:C)-induced protection of neonatal mice against intestinal *Cryptosporidium parvum* infection requires an additional TLR5 signal provided by the gut flora. J Infect Dis **2014**; 209:457–67.